CATALYTIC PROPERTIES AND MECHANISM STUDIES OF THE PEPQ PROLIDASE FROM *Escherichia coli*

A Thesis

by

MIN SUN PARK

Submitted to the Office of Graduate Studies of
Texas A&M University
in partial fulfillment of the requirements for the degree of

MASTER OF SCIENCE

August 2005

Major Subject: Chemistry

CATALYTIC PROPERTIES AND MECHANISM STUDIES OF THE PEPQ PROLIDASE FROM *Escherichia coli*

A Thesis

by

MIN SUN PARK

Submitted to the Office of Graduate Studies of
Texas A&M University
in partial fulfillment of the requirements for the degree of

MASTER OF SCIENCE

Approved by:

Chair of Committee,	Frank M. Raushel
Committee Members,	Paul A. Lindahl
	Coran M. Watanabe
Head of Department,	Emile A. Schweikert

August 2005

Major Subject: Chemistry

ABSTRACT

Catalytic Properties and Mechanism Studies of the PepQ Prolidase

from *Escherichia coli.* (August 2005)

Min Sun Park., B.S., Sogang University

Chair of Advisory Committee: Dr. Frank M. Raushel

The PepQ prolidase from *Escherichia coli* catalyzes the hydrolysis of dipeptide substrates with proline residues at the C-terminus. The PepQ gene has been cloned, overexpressed and the enzyme purified to homogeneity. The k_{cat} and k_{cat}/K_m values for the hydrolysis of Met-Pro are 109 s^{-1} and 8.4 x 10^5 M^{-1} s^{-1}, respectively. The enzyme also catalyzes the stereoselective hydrolysis of organophosphate triesters and organophosphonate diesters. A series of 16 organophosphate triesters with a *p*-nitrophenyl leaving group was assessed as substrates for this enzyme. The S_P-enantiomer of methyl phenyl *p*-nitrophenyl phosphate was hydrolyzed with a k_{cat} of 36 min^{-1} and a k_{cat}/K_m of 710 M^{-1} s^{-1}. The corresponding R_P-enantiomer was more slowly hydrolyzed with a k_{cat} of 0.4 min^{-1} and a k_{cat}/K_m of 11 M^{-1} s^{-1}. The PepQ prolidase can be utilized for the kinetic resolution of racemic phosphate esters. The PepQ prolidase was shown to hydrolyze the *p*-nitrophenyl analogs of the nerve agents GB (sarin), GD (soman), GF, and VX.

The pH-rate profiles for the wild-type *E. coli* prolidase using proline dipeptides as substrates were obtained. The roles of H346, H228, and E384 in the enzyme catalytic

mechanism were also investigated by obtaining the pH-rate profiles for the mutants H346N, H228N, and E384Q. In an effort to clarify the mechanistic role of the interaction of the α-amino group of Xaa-Pro with metal at the enzyme active site, comparisons of the hydrolytic activity for Ala-Pro and 1-(1-oxopropyl)-L-proline, in which a hydrogen replaces the α-amino group of Ala-Pro, were performed.

DEDICATION

To my wife Kyoungsun for her love, understanding and constant support;

To my father and mother for their endless effort;

To my daughter Hyeri for the missed time we should share;

and to God.

ACKNOWLEDGMENTS

I would like to acknowledge my advisor, Dr. Frank M. Raushel, for his constant guidance and support in my graduate career at Texas A&M University, and the members of my committee: Dr. Paul A. Lindahl and Dr. Coran M. Watanabe, for their constant support for my studies. I also would like to thank my former and current labmates.

TABLE OF CONTENTS

LIST OF TABLES

LIST OF FIGURES

FIGURE Page

CHAPTER I

INTRODUCTION

Proline is unique among the 20 natural amino acids found in proteins due to its cyclic structure. Since prolyl residues confer a conformational constraint on the structural aspects of peptides, only a few proteases are known that are able to recognize this residue specifically. Two distinct groups of proline-specific peptidases have been identified in a wide range of organisms. The first group contains enzymes which hydrolyze the Pro-Xaa bond while the second group consists of enzymes which specifically hydrolyze the Xaa-Pro bond. The former group, including lipases and esterases, belongs to a family of proteins with an α/β-hydrolase structural fold [1, 2]. The second group belongs to a family of metallo-proteases that have a pita-bread structural fold [3, 4]. The N-terminal and C-terminal domains of the pita-bread family of enzymes contain two α-helices and two antiparallel β-strands. This family of enzymes is further subdivided into type I and type II classes where the type II enzymes have an extra helical subdomain of approximately 60 residues inserted within the C-terminal domain [4]. The pita-bread family of enzymes includes methionine aminopeptidase (MetAP), proline aminopeptidase (PepP), and prolidase (PepQ). Methionine aminopeptidase removes the N-terminal methionine from proteins (Met-/-Xaa-), whereas proline aminopeptidase catalyzes the cleavage of the peptide bond between any N-terminal amino acid and a penultimate proline residue (NH_2-Xaa-/-Pro-

---

This thesis follows the style and format of *Biochemistry*.

Xaa-) in both short and long peptides. Prolidase is a ubiquitous enzyme, which hydrolyzes dipeptides with proline at the C-terminus (NH_2-Xaa-/-Pro-CO_2H). Although its natural function is not clear, it may involve the metabolism of proline-containing proteins during the degradation of cellular dipeptides and in the recycling of proline [5]. A deficiency of this enzyme in human results in abnormalities of skin and other collagenous tissues [6]. These three enzymes have different activities and substrate specificities. However, the amino acid residues that are used to coordinate the binuclear metal center are conserved [3, 7, 8, 9]. Two metal ions are coordinated in the active site by ligation to two aspartates, two glutamates, and a histidine residue. Two histidines on either side of the metal center are also conserved residues in the common binuclear metal center found in the pita-bread family of enzymes. A representation of the binuclear metal center found in the prolidase from *Pyrococcus furiosus* (*Pf*pro) is shown in **Figure 1**. In addition to the fundamental interest of proline specificity, prolidase has potential pharmaceutical applications. The enzyme may serve as a potential target for a prodrug strategy since it is differently expressed in melanoma compared to cell lines derived from other tissues [10]. Further, the prolidase also catalyzes the stereoselective hydrolysis of organophosphate and organophosphonate analogs of toxic chemical warfare agents [11].

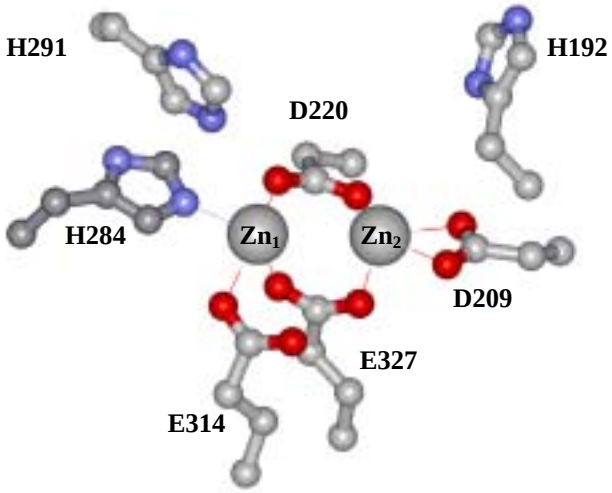

Figure 1: Structure of the binuclear metal center for the prolidase from *Pyrococcus furiosus*. The coordinates are taken from Maher et al. [9] and can be obtained from the Protein Data Bank (PDB) (1PV9).

CHAPTER II

CATALYTIC PROPERTIES OF THE PEPQ PROLIDASE FROM *Escherichia coli*

Organophosphate triesters are acetyl cholinesterase (AChE) inhibitors that exhibit high toxicity because of their ability to promote the accumulation of acetylcholine and the disruption of nerve transmission [12]. The reaction mechanism for the enzymatic hydrolysis of acetylcholine by AChE is shown in **Figure 2**. An active-site serine residue initiates a nucleophilic attack on the carbonyl carbon of acetylcholine to form a covalent acetyl-enzyme intermediate. The free enzyme is regenerated by a hydrolytic attack of water and release of acetate. Organophosphate triesters apparently mimic the natural substrate, forming a phosphoenzyme intermediate. However, the regeneration of the free enzyme through the nucleophilic attack by water on the phosphoenzyme intermediate is extremely slow. Nevertheless, organophosphates have been distributed extensively for the control of insects and other agricultural pests. The hazardous nature of these compounds and their broad usage has led to efforts for the development of improved methods for the destruction of these toxic substances. The catalytic detoxification of organophosphates was first reported by Mazur, who identified an enzyme from rabbit tissue with the ability to hydrolyze DFP, a structural analog of the nerve agents, sarin and soman [13]. In an effort to find safer and more effective alternatives to chemical degradation, attention has turned to the discovery of more proficient enzymes for the recognition and catalytic detoxification of organophosphate nerve agents.

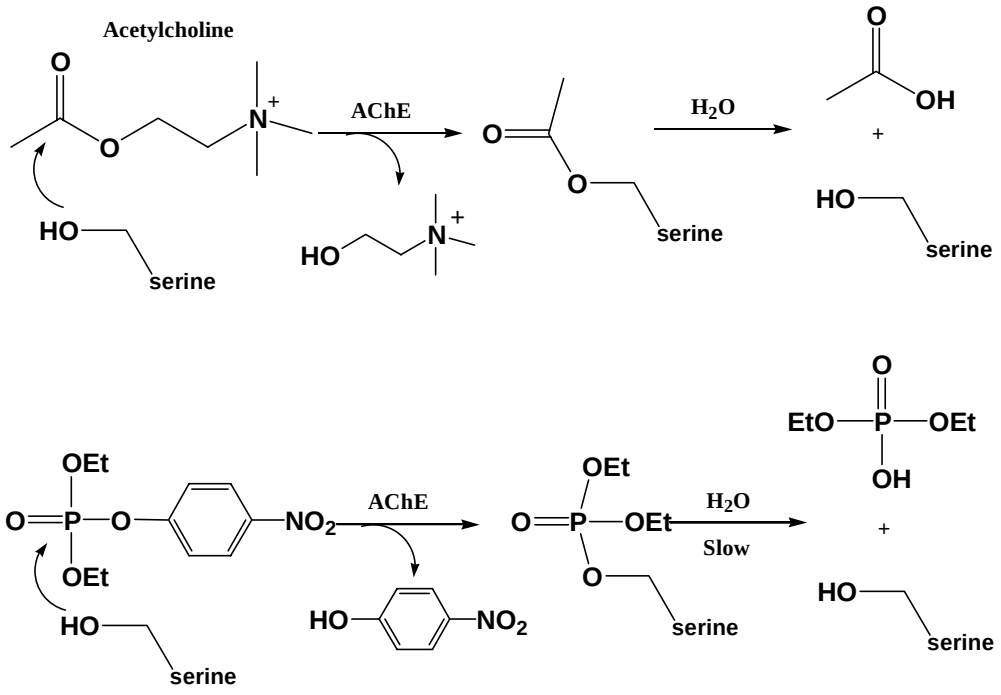

Figure 2: Reaction mechanism for the hydrolysis of acetylcholine by acetyl cholinesterase (AChE) and the inactivation of AChE by the organophosphate triester, paraoxon.

The amino acid sequences of MetAP, PepP, and PepQ have a high level of amino acid sequence similarity to organophosphorus acid anhydrolase (OpaA) from *Altermonas* sp. JD6.5. OpaA is capable of hydrolyzing organophosphorus compounds with P-O and P-F bonds. The amino acid sequence of OpaA is approximately 47% identical to that of the *E. coli* prolidase [7].

Organophosphorus acid anhydrolases are found in a wide variety of prokaryotes and eukaryotes [14, 15]. Although the natural function of these enzymes is not clear, these proteins may play an important role in the cellular metabolism of dipeptides. The organophosphorus acid anhydrolase, possessing a high level of hydrolytic activity toward diisopropyl fluorophosphate (DFP), was purified from *Altermonas* sp. strain JD6.5 [14, 16]. The catalytic activity of OpaA toward a series of organophosphate (see **Figure 3**) and organophosphonate analogs of toxic chemical warfare agents has been reported [17, 18].

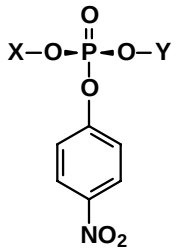

Figure 3: Structure of the organophosphate triester.

Materials and Methods

Materials. A library of chiral organophosphate compounds (**1-10**) was synthesized as previously described [19, 20, 21]. The structures, based upon the template shown in **Figure 3**, are presented in the Table on the page 7. The chiral analogs of VX (**11**) sarin (**12**) rVX (**13**), GF (**14**) and soman (**15**) were prepared according to established protocols [22]. The structures of these compounds are presented in **Figure 4**. These organophosphonates are extremely toxic and should be used with the appropriate safeguards. DFP was purchased from Sigma. Wizard Genomic DNA purification kits were purchased from Promega. The gel extraction kit was obtained from QIAGEN. Restriction enzymes and T4 DNA ligase were acquired from New England BioLabs. The Xaa-Pro dipeptides listed in **Table 3** were purchased from TCI America.

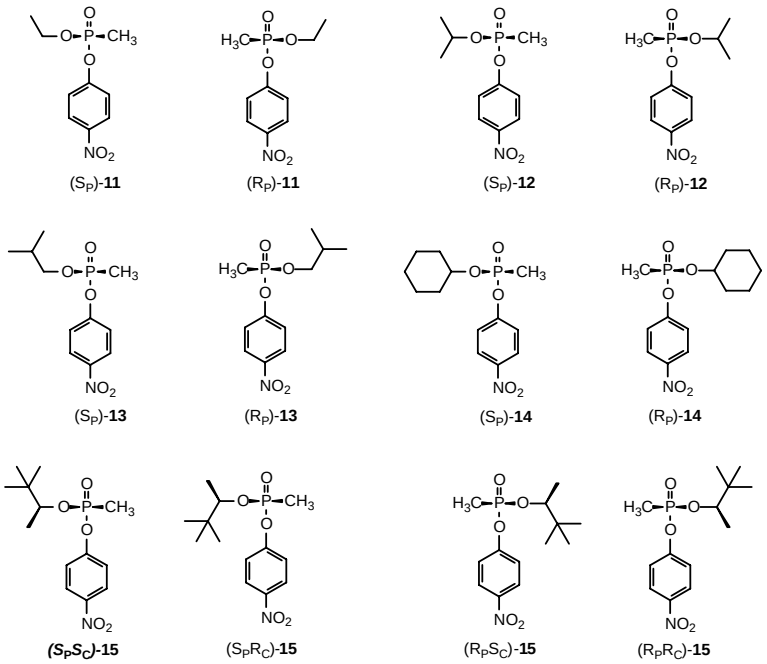

Figure 4. The structures of the organophosphonate compounds.

*Cloning of pepQ Gene***.** Chromosomal DNA from *E. coli* BL21 (DE3) was purified with a commercial kit (Promega) and used as a template for the amplification of the *pep*Q gene using the polymerase chain reaction (PCR). PCR was carried out using two sets of primers, designed on the basis of the sequence deposited in GenBank (X54687). The sequence for the first primer was 5'-GGAATTAAGCTTAAGGAGATATACATATGGAATCACTGGCCTCG-3' while the sequence for the second primer was 5'-CCGGAATTCTTATTCTTCAATCGCTAACA-3'. The first primer included a *Hin*dIII restriction site and a ribosomal binding site. The second primer included an *Eco*RI site. PCR fragments were digested with *Hin*dIII and *Eco*RI and then subcloned into a pBluescript SK+ vector. The recombinant pBluescript vector was transferred to the host *E. coli* BL21 strain. The DNA sequence of the cloned *pep*Q gene was confirmed by the Gene Technology Laboratory at Texas A&M University.

Purification of PepQ. The *E. coli* culture was grown at 37 ^{o}C in 2 liters of LB media in the presence of ampicillin (50 mg/L). Protein expression was induced by the addition of 0.5 mM IPTG after 6 hours. Incubation was continued at 37 ^{o}C for another 10 hours. The cells were harvested by centrifugation and suspended in 50 mM HEPES buffer (pH 8.5). After disrupting the cells by ultra-sonication for 40 minutes, the cell debris was removed by centrifugation and the supernatant solution was fractionated with $(NH_4)_2SO_4$ at 70 % saturation. After centrifugation, the pellet was dissolved in 50 mM HEPES buffer (pH 8.5) containing 0.1 mM $MnCl_2$ and loaded onto a Superdex-200 column. The catalytically active fractions were applied to a Q-Sepharose column and

eluted from the column with a linear gradient of 50 mM HEPES buffer (pH 8.5) containing 1.0 M NaCl. Fractions containing the enzyme were concentrated and loaded onto the Superdex-200 column to remove NaCl. SDS gel electrophoresis indicated that the purity of the prolidase was >95%. The purified protein was subjected to N-terminal amino acid sequence analysis. The sequence obtained for the first five residues, ***M E S L A***, agreed with the published gene sequence. The elution profile from a calibrated gel-filtration column was consistent with the formation of a dimer in solution.

Enzyme Assays. The activity of prolidase with a series of Xaa-Pro dipeptides was monitored by following the change in absorbance at 222 nm for the hydrolysis of the peptide bond using an extinction coefficient of 904 M^{-1} cm^{-1}. The assays were conducted in a volume of 1.0 mL in 10 mM Tris-HCl buffer, pH 8.0, using a Gilford 260 UV-vis spectrophotometer at 25 ^{o}C. The initial velocities for the enzymatic hydrolysis of the series of organophosphate triesters (**1-10**) and organophosphonate diesters (**11-15**) were conducted by measuring the change in absorbance at 400 nm for the release of *p*-nitrophenol. Each 3.0 mL assay contained 50 mM HEPES buffer, pH 8.0, 0.1 mM $MnCl_2$, 10 % (v/v) methanol, substrate and various amounts of PepQ. The full time courses for the enzymatic hydrolysis of racemic mixtures of organophosphates and phosphonates were monitored by following the absorbance change for the complete hydrolysis of both enantiomers using variable enzyme concentrations. The total substrate concentration was determined by hydrolysis of all enantiomers with KOH. The hydrolysis of DFP was monitored by following the release of fluoride.

Data Analysis. The steady state initial velocities for the hydrolysis of dipeptides, organophosphates (**1-10*)***, and organophosphonates (**11-15**) were fit to equation 1. In this equation k_{cat} is the turnover number, K_m is the Michaelis constant, A is the substrate concentration and E_t is the total enzyme concentration. The full time courses that exhibited single and double exponential phases were fit to equations 2 and 3, respectively. For these equations, A_1 and A_2 are the substrate concentrations for each enantiomer, k_1 and k_2 are the first-order rate constant for each phase, and *t* is time. The kinetic constants and the associated errors were obtained by fitting the data to the appropriate equation using SigmaPlot.

$$v / E_t = k_{cat} A / (K_m + A) \quad (1)$$

$$y = A_1(1 - e^{-kt}) \quad (2)$$

$$y = A_1(1 - e^{-k_1 t}) + A_2(1 - e^{-k_2 t}) \quad (3)$$

Results

Cloning and Sequencing of pepQ Gene. The *pep*Q gene from the BL21 strain of *E. coli* was sequenced and found to contain a stop codon after 1329 nucleotides. Therefore, the prolidase is expected to contain 443 amino acids. The DNA sequence from BL21 matched well with those of the *pepQ* gene from *E. coli* K12 (GenBank accession no. P21165) except for 24 differences at the third codon position. However, the derived amino acid sequence was exactly the same as for *E. coli* K12. The purified recombinant PepQ, cloned from *E. coli* BL21, has a molecular weight of ~50 kDa as determined from a calibrated SDS electrophoresis gel. The molecular weight of PepQ, based on the DNA sequence, is calculated to be 50,176.

*Hydrolysis of Dipeptides***.** The substrate specificity of the recombinant *E. coli* prolidase was evaluated using fourteen proline-containing dipeptides (**Table 1**). Significant catalytic activity occurred with dipeptides containing nonpolar amino acids at the N-terminal position. Dipeptides containing large hydrophobic side chains at the N-terminus have low K_m values and high values of k_{cat}/K_m. For example, Met-Pro has the lowest K_m value of 0.13 mM and the highest value for k_{cat}/K_m of 8.4×10^5 M^{-1} s^{-1}.

Table 1: Kinetic constants for the hydrolysis of Xaa-Pro dipeptides at pH 8.0 and 25°C.

Substrate	k_{cat}/K_m (M^{-1} s^{-1})	k_{cat} (s^{-1})	K_m (mM)
Ala-Pro	6.5 (0.5) x 10^4	120 ± 30	1.9 ± 0.5
Leu-Pro	2.1 (0.05) x 10^5	215 ± 25	1.0 ± 0.1
Gly-Pro	2.5 (0.1) x 10^4	34 ± 1	1.4 ± 0.2
Phe-Pro	4.6 (0.3) x 10^5	200 ± 20	0.43 ± 0.06
Met-Pro	8.4 (0.8) x 10^5	109 ± 7	0.13 ± 0.01
Val-Pro	1.6 (0.1) x 10^5	64 ± 7	0.40 ± 0.07
His-Pro	8.2 (0.3) x 10^5	123 ± 5	0.15 ± 0.01
Tyr-Pro	7.1 (0.3) x 10^5	116 ± 6	0.16 ± 0.01
Ser-Pro	6.0 (0.3) x 10^5	281 ± 25	0.46 ± 0.06
Ile-Pro	5.7 (0.4) x 10^5	57 ± 3	0.10 ± 0.01
Lys-Pro	8.8 (0.5) x 10^5	240 ± 11	0.27 ± 0.02
Pro-Pro	4.1 (0.3) x 10^5	129 ± 15	0.31 ± 0.05
Arg-Pro	1.4 (0.1) x 10^6	142 ± 5	0.10 ± 0.01
Trp-Pro	N/A	N/A	N/A

*Hydrolysis of Organophosphates***.** The prolidase from *E. coli* has a broad substrate specificity toward the hydrolysis of organophosphate triesters (**Table 2**). The active site within the PepQ *E. coli* prolidase can accommodate a variety of bulky side chains attached to the phosphorus center. In addition, the enzyme exhibits a marked stereoselectivity toward the hydrolysis of chiral *p*-nitrophenyl phosphotriester substrates with a clear preference for the S_P-enantiomer over the R_P-enantiomer. The physically smaller substituent is preferentially found at the *pro*R position (denoted by **X** in **Figure 3**) while the physically larger substituent is preferentially attached to the *pro*S position (denoted by **Y** in **Figure 3**). The stereoselectivity ranges from ~60 for the discrimination between phenyl and methyl substituents to ~1 for the discrimination between isopropyl and phenyl substituents.

The catalytic constants are influenced by the specific substituents attached to the phosphorus center. Those substrates with a methyl substituent at the *pro*R position (**X** in **Figure 3**) have the highest values of k_{cat} and k_{cat}/K_m. The values of k_{cat} are reduced when the methyl group is replaced by other substituents. For example, (S_P)-methyl phenyl *p*-nitrophenyl phosphate (**4**) has a higher k_{cat} value, compared to the values measured for either (S_P)-ethyl phenyl *p*-nitrophenyl phosphate (**7**) or (S_P)-isopropyl phenyl *p*-nitrophenyl phosphate (**9**), which are reduced by 60- and 257-fold, respectively. The enzyme exhibits the highest value of k_{cat}/K_m for (S_P)-methyl phenyl *p*-nitrophenyl phosphate (**4**) and the lowest for (R_P)-ethyl isopropyl *p*-nitrophenyl phosphate (**6**). The enzyme exhibited a clear stereoselective preference for the S_p-enantiomer over the R_p-enantiomer when the substrate has a methyl substituent at the phosphorus center.

However, the chiral selectivity is essentially eliminated upon replacement of the methyl substituent with other groups, and the loss of stereoselectivity is also accompanied by poor overall kinetic parameters.

Hydrolysis of Organophosphonates. The catalytic activity of the prolidase from *E. coli* was also tested with a variety of methyl phosphonates that are analogs of the nerve agents, sarin (**12**), soman (**15**) GF (**14**), VX (**11**), and rVX (**13**). The kinetic constants are presented in **Table 3**. For this set of substrates, the R_P-configuration at the phosphorus center is clearly preferred over the S_p-configuration. However, the relative stereochemical preference (with regard to the orientation of the large and small substituents) is the same as it is for the corresponding series of organophosphate substrates. The best of the methyl organophosphonate substrates is the R_P-enantiomer of the rVX analog (**13**) and the worst is the S_P-enantiomer of the GF analog (**14**). The organophosphonate compounds containing a bulky carbon center within one substituent exhibited greater stereoselectivity. For example, the R_P-enantiomers of the VX (***11***) and rVX (**13**) analogs are 2 and 11 times faster than the corresponding S_P-enantiomers, whereas the R_p-enantiomers of the analogs for sarin (**12**) and GF (**14**) are hydrolyzed 94 and 121 times faster than the corresponding S_P-enantiomers.

Table 2: Kinetic constants for the hydrolysis of organophosphates at pH 8.0, 25°C.

Substrate	X	Y	k_{cat} (min^{-1})	k_{cat}/K_m ($M^{-1}s^{-1}$)	K_m (mM)
1	CH_3	CH_3	0.56 ± 0.06	7.2 ± 0.5	1.3 ± 0.2
(R_P)-**2**	CH_2CH_3	CH_3	0.36 + 0.04	2.6 ± 0.2	2.3 ± 0.4
(S_P)-**2**	CH_3	CH_2CH_3	39 ± 1	105 ± 3	6.2 + 0.8
(R_P)-3	$CH(CH_3)_2$	CH_3	0.15 ± 0.01	4.8 ± 0.3	0.51 + 0.07
(S_P)-**3**	CH_3	$CH(CH_3)_2$	12 ± 1.3	100 ± 8	2.0 ± 0.3
(R_P)-**4**	C_6H_5	CH_3	0.40 ± 0.03	11 ± 1	0.58 ± 0.07
(S_P)-**4**	CH_3	C_6H_5	36 ± 4	707 ± 42	0.9 + 0.1
5	CH_2CH_3	CH_2CH_3	1.2 ± 0.1	3.2 ± 0.1	6.2 ± 0.5
(R_P)-**6**	$CH(CH_3)_2$	CH_2CH_3	0.12 ± 0.01	1.1 ± 0.06	1.8 ± 0.3
(S_P)-**6**	CH_2CH_3	$CH(CH_3)_2$	0.59 ± 0.06	8.3 ± 0.6	1.2 ± 0.2
(R_P)-**7**	C_6H_5	CH_2CH_3	0.22 ± 0.02	4.6 ± 0.2	0.8 ± 0.1
(S_P)-**7**	CH_2CH_3	C_6H_5	0.6 ± 0.1	28 ± 2	0.37 + 0.06
8	$CH(CH_3)_2$	$CH(CH_3)_2$	1.0 ± 0.1	1.7 ± 0.1	10 ± 1
(R_P)-9	C_6H_5	$CH(CH_3)_2$	0.05 ± 0.01	9.5 + 0.3	0.09 ± 0.01
(S_P)-**9**	$CH(CH_3)_2$	C_6H_5	0.17 ± 0.02	8.1 ± 0.4	0.30 ± 0.05
10	C_6H_5	C_6H_5	0.05 ± 0.01	6.9 ± 0.5	0.13 ± 0.02

Table 3: Kinetic constants for the hydrolysis of organophosphonates at pH 8.0, 25 ^{o}C.

Substrate	k_{cat} (min^{-1})	k_{cat}/K_m ($M^{-1}s^{-1}$)	K_m (mM)
(S_P)-**11**	1.6 ± 0.1	8.1 ± 0.3	3.3 ± 0.4
(R_P)-**11**	3.4 + 0.3	17 ± 1.7	3.3 ± 0.5
(S_P)-**12**	0.07 ± 0.01	0.32 ± 0.01	3.7 ± 0.5
(R_P)-**12**	2.3 ± 0.2	30 ± 1.6	1.3 ± 0.2
(S_P)-**13**	2.7 ± 0.2	20 + 1.7	2.3 ± 0.3
(R_P)-**13**	134 ± 27	218 ± 6	10 ± 2
(S_P)-**14**	nd	0.6 ± 0.1	nd
(R_P)-**14**	45 ± 7	73 + 3	10 ± 2
(S_PS_C)-**15**	0.010 ±0.001	0.07 ± 0.01	2.3 ± 0.5
(S_PR_C)-**15**	0.040 ± 0.01	0.11 ± 0.01	5.9 ± 0.6
(R_PS_C)-**15**	33 ± 2	427 ± 16	1.1 ± 0.1
(R_PR_C)-**15**	5.0 ± 0.04	30 ± 2	2.7 ± 0.3

The most extreme example of stereoselectivity is observed among the four analogs of soman (**15**) where there is an additional stereogenic carbon center within the O-pinacolyl substituent. The stereochemical preference for the four soman analogs is as follows: $R_pS_c > R_pR_c > S_pR_c > S_pS_c$. These results indicate that the R_p-configuration is preferred relative to the S_p-configuration whereas the preference for the configuration at the carbon center is dependent on configuration at the phosphorus center. The stereoselective preference for the phosphorus center is high, but the difference in the catalytic constants for the chiral carbon center within the O-pinacolyl group is relatively small. The R_pS_c-diastereomer of **15** is preferred by a factor of 6100 over the S_pS_c-diastereomer.

Hydrolysis of DFP. The hydrolysis of the P-F bond in DFP is faster than the P-O bond in the organophosphate triesters and organophosphonate diesters tested for this investigation. The values for k_{cat}, k_{cat}/K_m, and K_m for the hydrolysis of DFP are 590 min^{-1}, 250 M^{-1} s^{-1}, and 38 $\pm$ 17 mM, respectively. The value of k_{cat}/K_m for the hydrolysis of DFP is ~150-fold higher than that for the hydrolysis of diisopropyl *p*-nitrophenyl phosphate (**8**).

Discussion

The PepQ prolidase from *E. coli* catalyzes the hydrolysis of dipeptides possessing a proline residue at the C-terminus. The enzyme also catalyzes the stereoselective hydrolysis of phosphate and phosphonate esters but the turnover numbers for the dipeptides are significantly greater than for the phosphorus containing esters. The hydrolysis of Met-Pro, for example, is hydrolyzed more than three orders of magnitude faster than (S_p)-methyl phenyl *p*-nitrophenyl phosphate (**4**), the organophosphate substrate with the largest k_{cat}/K_m. The proline amino peptidase (PepP) from *E. coli* has also been reported to cleave a limited number of dipeptides (Xaa-Pro) [23]. However, the catalytic activity with dipeptides is considerably slower than the turnover numbers for longer peptides. Proline aminopeptidase preferentially hydrolyzes longer polypeptides and is able to distinguish among amino acids that occupy the third and forth amino acids from the N-terminus of the substrate [25]. The PepP and PepQ prolidases from *E. coli* are from the same enzyme superfamily and thus the amino acid residues that are used to coordinate the binuclear metal centers are conserved but the specific residues that define the substrate binding pockets are different. Recently, the three-dimensional structure of the prolidase from *Pyrococcus furiosus,* that is analogous to PepQ, has been solved and the structural similarity within the active sites of this superfamily has been confirmed [25].

The PepQ prolidase from *E. coli* hydrolyzes the *p*-nitrophenyl analogs of the organophosphorus nerve agents GB, GD, GF, VX, and rVX. The enzyme stereoselectively hydrolyzes organophosphonate esters with a preference for the R_p-

configuration of the substrates tested for this investigation (**Table 3**). This stereoselectivity is similar to that previously observed for OpaA [14]. However, the prolidase from *E. coli* exhibits a more restricted stereoselectivity and a reduced rate of hydrolysis for organophosphonate esters. The k_{cat}/K_m value for the R_PS_C diastereomer of **15** with PepQ is two orders of magnitude slower than the value previously measured for OpaA. Likewise, the k_{cat}/K_m value for the hydrolysis of the R_P-enantiomer of **12** is approximately an order of magnitude slower than the value previously measured for OpaA.

The bacterial phosphotriesterase (PTE) is another enzyme with a demonstrated potential for utilization in the catalytic decomposition of chemical warfare agents. This enzyme has a similar stereoselectivity to that displayed by PepQ for the set of *p*-nitrophenyl analogs of the nerve agents **11**-**15** (**Table 3**) and the organophosphates **1**-**10** (**Table 2**) [26, 20, 28]. However, the overall kinetic parameters obtained with PTE for these substrates are significantly higher than found in this study for PepQ. For example, the k_{cat}/K_m values for (S_p)- and (R_p)-methyl ethyl *p*-nitrophenyl phosphate (**2**) with PTE are 10^4 and 10^5 -fold higher than for prolidase, respectively [27]. The stereochemical selectivity of prolidase for the organophosphates with a methyl substituent (e.g. **2**, **3**, and **4**), is higher than that of PTE. However, the remaining *p*-nitrophenyl organophosphates have a similar degree of stereoselectivity as does PTE.

CHAPTER IV

PH DEPENDENCE OF ENZYMATIC HYDROLYSIS BY THE PEPQ PROLIDASE FROM *Escherichia coli*

Since the pita-bread family of enzymes have a similar function (cleavage of a peptide bond) and a similar binuclear metal center, it is reasonable to infer that these enzymes share a common mechanism. The biochemical and structural analysis of methionine aminopeptidase (MetAP), proline aminopeptidase (PepP), and *Pyrococcus furiosus* prolidase (*Pf*pro) suggests that the substrate binds to the dinuclear metal center within the active site, and it may activate a metal-bridging water to attack the scissile bond. Hydrogen bonds established to the substrate by two histidines may stabilize the transition state of a noncovalent *gem*-diolate tetrahedral intermediate. The significant reduction of activity of the two-histidine mutants of MetAP and PepP suggests that these two histidines may play an important role for the enzyme catalytic activity [29,30,31].

In vitro prolidase is most active in the presence of Mn^{2+} ions, and recently, EPR spectroscopic measurements have shown that both metals in the active site are manganese in the +2 oxidation state (unpublished results). The two metals are bridged by a water or hydroxide ion. The binuclear metal cluster may provide a substrate-binding site with the stabilization of the transition state and/or the activation of a nucleophile for the catalytic reaction. In previous studies on the catalytic properties of the prolidase from *E. coli*, the enzyme exhibited significant catalytic activity toward the hydrolysis of Xaa-Pro dipeptides containing nonpolar amino acids at the N-terminal position [11].

The structure of the MetAP from *E. coli* with the reaction product methionine and a phosphorus-containing transition state analog was determined by X-ray crystallography [32] in **Figure 5**. The reaction products and transition state analogs bind to the active site in a similar manner. The N-terminus ligates to Co_2, and an oxygen atom of the phosphonate or carboxylate is bridged between Co_1 and Co_2. His178 and His79 have hydrogen bonds to the oxygen atoms of the inhibitors.

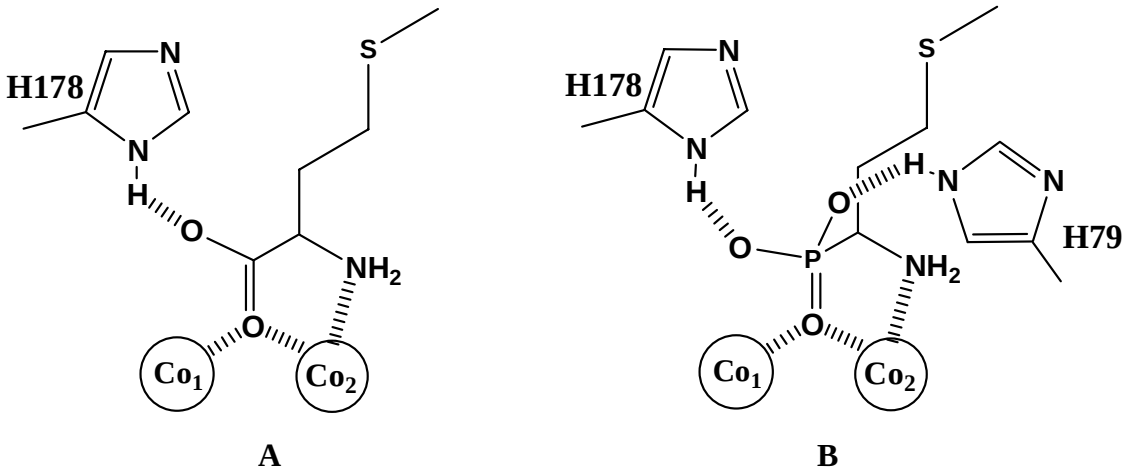

Figure 5: Models of the binding mode of a phosphonate and carboxylate ligand in the active site of MetAP from *E. coli*. The coordinates are taken from W. T. Lowther et al. [29] and can be obtained from the PDB (1C21 and 1C24).

The X-ray structure of the prolidase from *Pyrococcus furiosus* (*Pf*pro) was recently solved in the presence of the inhibitor, (2S, 3R)-3-amino-2-hydroxyl-5-methyl-hexanoyl-1-proline (AHMH-Pro), which resembles Xaa-Pro [9]. The AHMH-Pro is a dipeptide with a β-amino acid and a hydroxyl substituent at the α-position of leucine. The carbonyl oxygen from the proline moiety is coordinated to M_A, the hydroxyl group at C-2 displaces the hydroxide that bridges the two divalent cations and the amino group from C-3 coordinates to M_B. His-192 and His-291 form hydrogen bonds with the C-terminal carboxylic acid and the carbonyl oxygen of the bound inhibitor, respectively. The binuclear metal-inhibitor complex of *Pf*pro is shown in **Figure 6**.

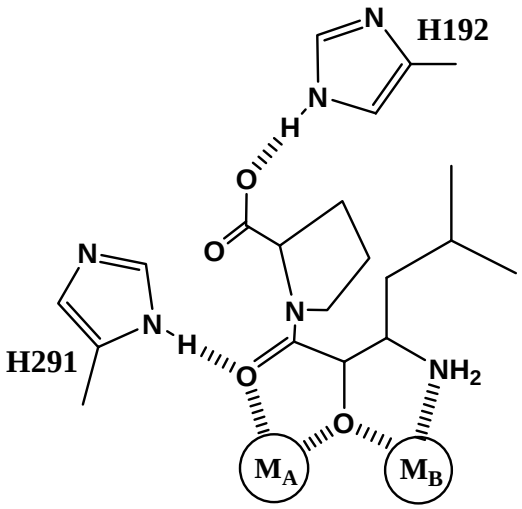

Figure 6: The model of *Pf*pro-inhibitor (AHMH-Pro) complex obtained from M. J. Maher et al. [9].

Materials and Methods

Materials. Met-Pro, and Ala-Pro were purchased from Sigma. 1-(1-oxopropyl)-L-proline was purchased from TimTec Stock Library. The structure of 1-(1-oxopropyl)-L-proline is presented in **Scheme 1**. QuickChange site-directed mutagenesis kit was purchased from Stratagene. Wizard Genomic DNA purification kits were purchased from Promega. The gel extraction kit was obtained from QIAGEN. The Gene Technology Laboratory at Texas A&M University performed oligonucleotide primer synthesis and DNA sequencing reactions.

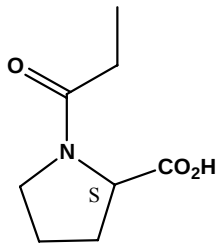

Figure 7. The structure of the 1-(1-oxopropyl)-L-proline

Site-Directed Mutagenesis. Site-directed mutagenesis was performed using the QuickChange site-directed mutagenesis kit. Primers of 32 bases (5'-CCGCTGGGCCTGCAGGTGAATGACGTCGCTGG-3') and 29 bases (5'-CGCTGCGGTGCTGAATTACACCAAACTGG-3') were used to change the His346 and His228 codon (CAT) to the Asn codon (AAT). Primers of 28 bases (5'-GGTGTTAACCATCCAACCGGGTATCTAC-3') were used to change the Glu384 codon (GAA) to the Gln codon (CAA). The DNA was transformed into XL1-Blue cells. The mutated plasmids were sequenced to ensure the fidelity of the PCR reactions. Well-

isolated colonies of the XL1-Blue cells from a fresh Luria-Bertani (LB) agar plate containing antibiotic were purified by Wizard Plus SV Miniperps DNA purification System, and they were introduced into competent BL21 cells by transformation.

Purification of PepQ. The *E. coli* culture was grown at 37 ^{o}C in 2 liters of LB media in the presence of ampicillin (50 mg/L). Protein expression was induced by the addition of 0.5 mM IPTG after 6 hours. Incubation was continued at 37 ^{o}C for another 10 hours. The cells were harvested by centrifugation and suspended in 20 mM HEPES buffer (pH 8.5). After disrupting the cells by ultra-sonication for 40 minutes, the cell debris was removed by centrifugation and the supernatant solution was fractionated with $(NH_4)_2SO_4$ at 70 % saturation. After centrifugation, the pellet was dissolved in 20 mM HEPES buffer (pH 8.5) and loaded onto a Superdex-200 column. The catalytically active fractions were applied to a Q-Sepharose column and eluted from the column with a linear gradient of 20 mM HEPES buffer (pH 8.5) containing 1.0 M NaCl. Fractions containing the enzyme were concentrated and loaded onto the Superdex-200 column to remove NaCl. SDS gel electrophoresis indicated that the purity of the prolidase was >95%.

Kinetic Measurements and Data Analysis. The purified wild-type and mutant prolidase were activated by incubating the enzyme in 0.1 mM $MnCl_2$ for 48h at 4^{o}C. The activated wild-type or mutant prolidases were assayed by measuring the change in absorbance at 222 nm for the hydrolysis of the peptide bond (ϵ = 904 M^{-1} cm^{-1}). The assays were conducted in a micro-plate using a SPECTRAmax-340 spectrometer at 25 ^{o}C. The kinetic parameters, k_{cat} and k_{cat}/K_m, were determined by fitting the initial velocity

data to equation 1, where v is the initial velocity, k_{cat} is the turnover number, K_m is the Michaelis constant, A is the substrate concentration and E_t is the total enzyme concentration.

$$v / E_t = k_{cat} A / (K_m + A) \quad (1)$$

The pH-rate profiles were also determined for the wild-type and mutant pepQ prolidase with Met-Pro. The wild-type enzyme was also used for the pH-rate profiles with 1-(1-oxopropyl)-L-proline and Ala-Pro. Buffers (10 mM) were brought to the correct pH with NaOH and HCl. The buffers included the following: MES (5.0-6.75), HEPES (7.0-8.25), TEBS (8.5-9.5), CHES (9.75-10.0). The final pH was measured at the end of the enzyme-catalyzed reaction. The pK_a values from the pH-rate profiles were determined by fitting the data to equation 2, 3 or 4, where y is k_{cat} or k_{cat}/K_m, c is the pH independent value of y, H is the hydrogen-ion concentration, and K_a and K_b are the dissociation constants of the ionizable groups.

$$\log y = \log[c/(1 + H/K_a)] \quad (4)$$

$$\log y = \log[c/(1 + H/K_a + K_b/H)] \quad (5)$$

$$\log y = \log[c/(1 + H^2/K_a^2 + K_b/H)] \quad (6)$$

Results

Kinetic Parameters of the Wild-type and Mutant Prolidases for Dipeptide. The values of k_{cat}, K_m, and k_{cat}/K_m for the hydrolysis of the Met-Pro dipeptide at pH 8.0 and 25 ^{o}C are listed in **Table 4** for the wild-type, H228N, H346N, H346A, and E384Q mutants of *E. coli* prolidase. The activities of the mutants H228N, H346N, and E384Q toward Met-Pro are reduced. For example, the values of k_{cat}/K_m of H228N, H346N, H346A, and E384Q are reduced by ~50-, 80-, 280-, and 110-fold, respectively. The mutant enzymes also have higher K_m values compared to that of the wild-type enzyme. The kinetic constants suggest that the function of His228, His346, and Glu384 are important but not absolutely essential for catalytic activity. The significant decrease in the activity of the mutant H346A compared to the mutant H346N shows that the hydrogen bond in the enzyme-substrate complex plays an important role during the hydrolysis.

The hydrolysis of 1-(1-oxopropyl)-L-proline with wild-type enzyme displayed a dramatically lower activity than that of Ala-Pro dipeptide. The specific activity of the wild-type enzyme with 1-(1-oxopropyl)-L-proline was less than 7.2 x 10^{-4} sec^{-1}, which reveals 6 x 10^{-4} % of the activity with Ala-Pro. The result indicates that the α-amino group of Xaa-Pro dipeptides is required for the enzyme-catalyzed reaction.

Table 4: Kinetic constants for the hydrolysis of Met-Pro dipeptide at pH 8.0 and 25 ^{o}C.

Prolidase	k_{cat}/K_m (M^{-1} s^{-1})	k_{cat} (s^{-1})	K_m (mM)
Wild-type	8.4 (0.8) x 10^5	109 ± 7	0.13 ± 0.01
H228N	1.8 (0.3) x 10^4	11 ± 3	0.6 ± 0.2
H346N	1.1 (0.2) x 10^4	5.4 ± 0.5	0.5 ± 0.07
H346A	3.0 (0.2) x 10^3	1.0 ± 0.5	3.2 ± 2.0
E384Q	7.9 (1.5) x 10^3	2.8 ± 0.4	0.36 ± 0.09

pH-Rate Profiles of the Wild-type, Mutant H228N, H346N, and E384Q for Met-Pro Dipeptide. The pH dependence of the kinetic parameters, k_{cat} and k_{cat}/K_m, of the wild-type, H228N, H346N, and E384Q mutants of prolidase were determined with Met-Pro as a substrate. The plots of log k_{cat} and log k_{cat}/K_m against pH are shown in **Figure 8,9**. The shape of the log k_{cat} profiles is identical to that of the log k_{cat}/K_m profiles. The pK_a values of the log k_{cat} and log k_{cat}/K_m profiles of the wild-type and H228N, H346N, and E384Q mutants of prolidase obtained from fitting the plots to eq 3 and 4 are shown in **Table 5.**

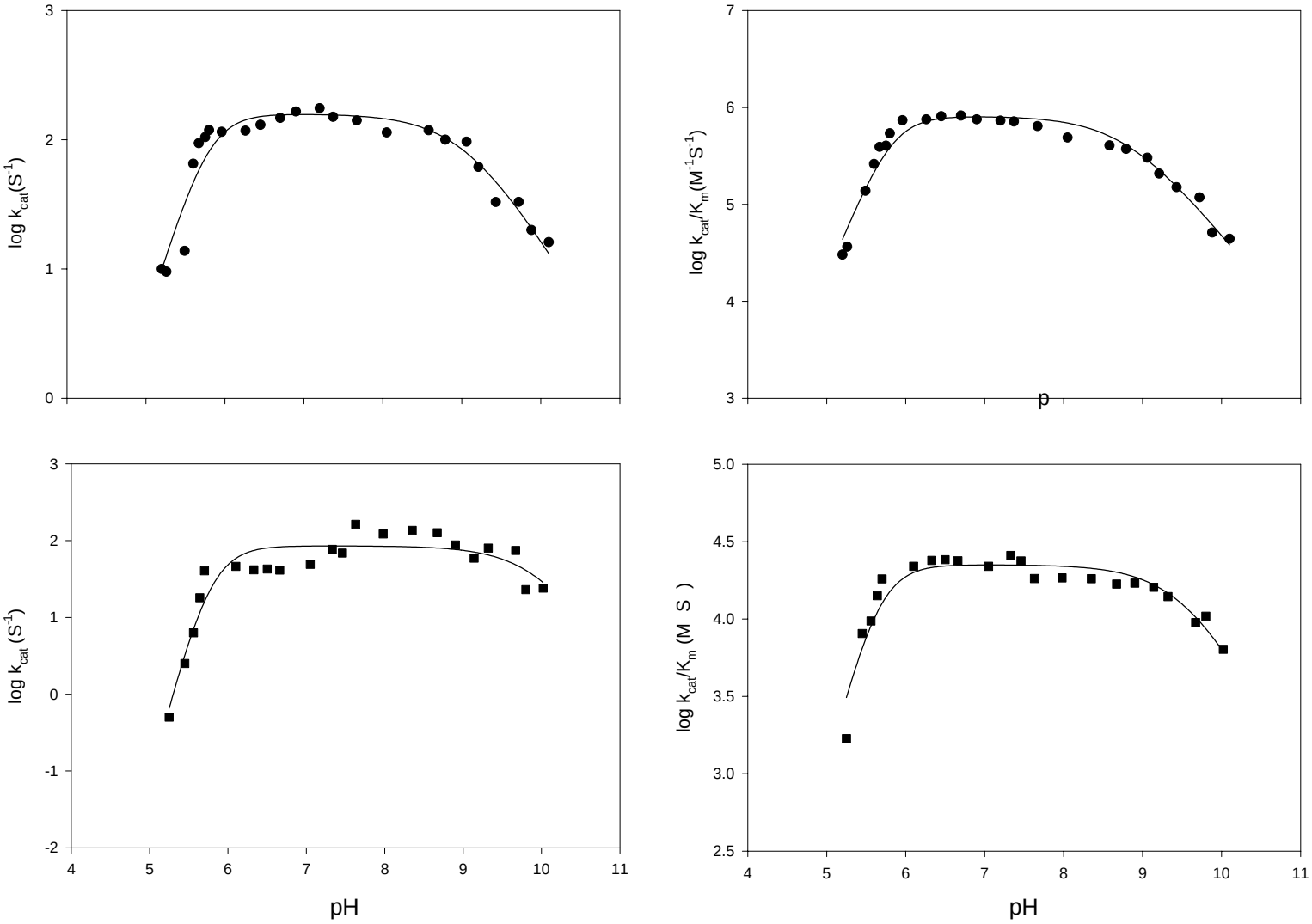

Figure 8: pH-rate profiles for the hydrolysis of Met-Pro with wild-type (●) and H228N (■).

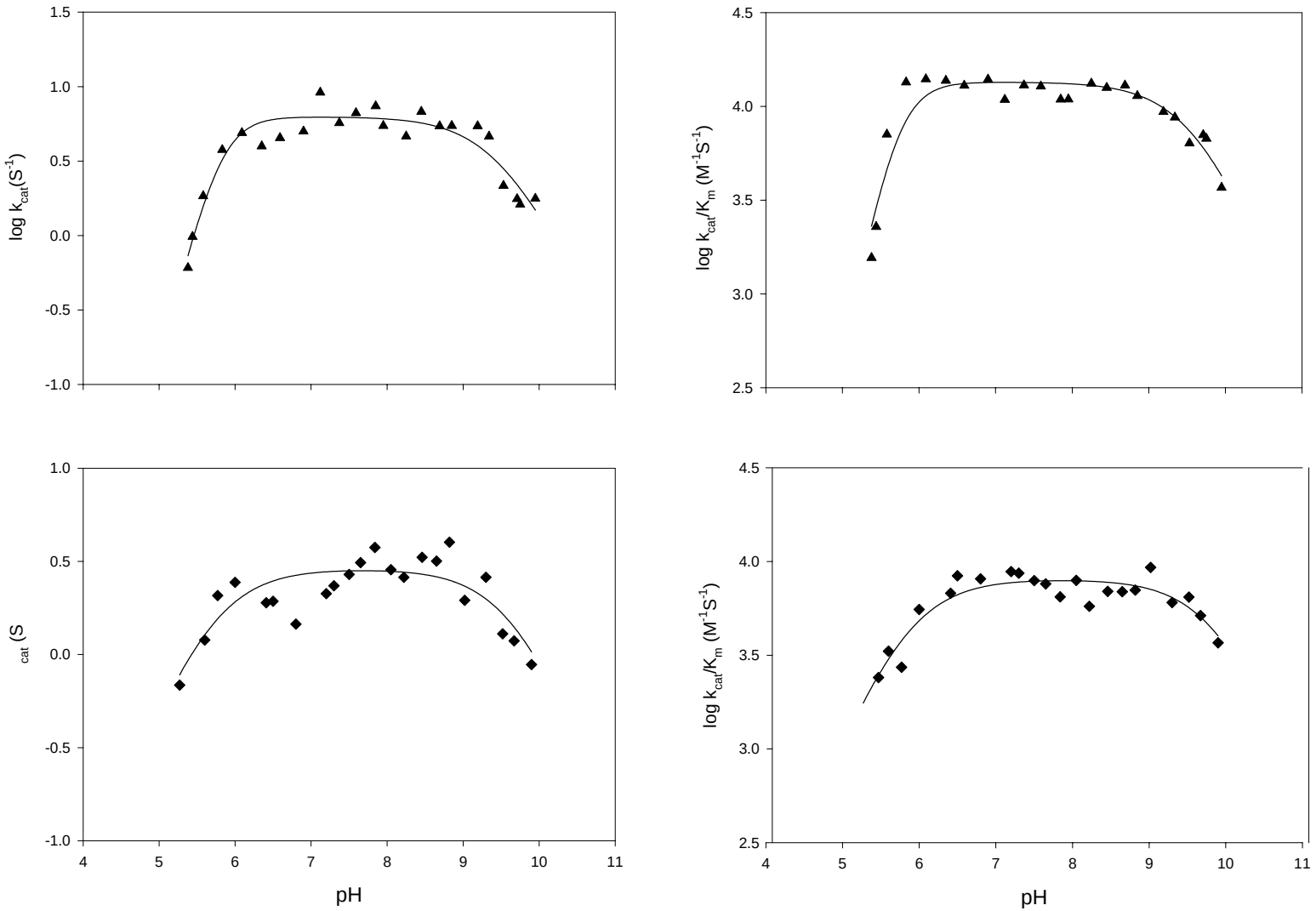

Figure 9: pH-rate profiles for the hydrolysis of Met-Pro with H346N (▲) and E384Q (♦).

Table 5. pK_a values of the log k_{cat} and log k_{cat}/K_m profiles for the hydrolysis of Met-Pro.

Prolidase	pK_a in low pH		pK_a in high pH	
	log k_{cat}/K_m	log k_{cat}	log k_{cat}/K_m	log k_{cat}
Wild-type	5.9 ± 0.09	5.8 ± 0.1	9.4 ± 0.1	9.1 ± 0.3
H228N	5.7 ± 0.06	5.8 ± 0.06	9.7 ± 0.4	9.2 ± 0.09
H346N	5.9 ± 0.06	6.0 ± 0.05	9.8 ± 0.2	9.7 ± 0.1
E384Q	5.9 ± 0.07	5.7 ± 0.07	9.4 ± 0.3	9.2 ± 0.3

The data of the wild-type enzyme were fit to eq 4. The slope of log k_{cat}/K_m profiles is approximately +2 at low pH, and –1 at high pH with pK_a values of 5.9 ± 0.09 and 9.4 ± 0.1, respectively. The pK_a values of the log k_{cat} profile are similar to these of log k_{cat}/K_m profiles. The plots indicate that the ionization of the two groups occurs with nearly identical pK_a values at low pH, and the ionization of another group occurs at high pH in the enzyme-catalyzed reaction.

The pH-rate profiles for the mutant H228N and H346N are similar in shape to that of the wild-type enzyme. The data were also fit to eq 4 for the log k_{cat} and log k_{cat}/K_m profiles with the mutants H228 and H346, which specifies ionization of three groups, two at low pH with similar pK_a values and one at high pH. The values of pK_a of log k_{cat}/K_m profile with the mutant H228 at the low pH and high pH were 5.7 ± 0.09 and 9.7 ± 0.4, respectively, which are similar to the values of wild-type enzyme. The log k_{cat}/K_m profile with H346N also shows similar pK_a values to that of wild-type enzyme.

However, the shape of the pH-rate profile for the mutant E384Q is different from that for the wild-type enzyme, which is a symmetrical bell plot. The diminution of the slope in the log k_{cat} and log k_{cat}/K_m profiles occurs with a slope of ~1 at low pH. It was fit to eq 3 with a pK_a of 5.9 ± 0.07 at low pH, and a pK_a of 9.4 ± 0.3 at high pH, indicating the ionization of two groups.

Kinetic Parameters of the Wild-type and Mutant Prolidases for Phosphotriester. The kinetic parameters of the mutants H228N, H346N, H346A, and E384 were determined for the hydrolysis of the phosphotriester substrate and the results are present in **Table 6**. The mutants H346A, H228N, and H346N hydrolyze the phosphotriester substrate are 2, 20, and 5 times faster than does the wild-type enzyme using k_{cat}/K_m as the kinetic parameter. However, when Glu384 is mutated to glutamine, the value of k_{cat}/K_m is reduced 16-fold. The results suggest that E384 enhances the enzyme catalytic activity for organophosphate hydrolysis while His228 and His346 are not involved in the hydrolysis of phosphotriesters. The value of k_{cat} of E384Q was not determined because of the high value of K_m for the hydrolysis of the substrate.

Table 6: Kinetic constants for the hydrolysis of diethyl *p*-nitrophenyl phosphotriester at pH 8.0 and 25 ^{o}C.

Prolidase	k_{cat}/K_m (M^{-1} s^{-1})	k_{cat} (min^{-1})	K_m (mM)
Wild-type	3.2 ± 0.1	1.2 ± 0.1	6.2 ± 0.5
H346N	14 ± 1	6.2 ± 0.7	8.9 ± 0.8
H346A	5.2 ± 0.5	2.0 ± 0.2	6.5 ± 1.0
H228N	61 ± 2	32 ± 2	8.8 ± 0.7
E384Q	0.2 ± 0.02	N/A	N/A

pH-Rate Profiles of the Wild-type, Mutants H228N, H346N, and E384Q for Phosphotriester. The log k_{cat} and log k_{cat}/K_m versus pH-rate profiles for the hydrolysis of diethyl *p*-nitrophenyl phosphotriester are presented in **Figure 10,11,** and the pK_a values in **Table 7** for the wild-type and H228N, H346N, and E384Q mutants. The shapes of the pH-rate profiles are similar, which are half-bell plots. The data for the mutant H228N were fitted to eq 2 and correspond to a pK_a of 7.8 ± 0.06 for log k_{cat}/K_m profile, which is somewhat higher than the pK_a of log k_{cat}/K_m profile for the hydrolysis of Met-Pro at the low pH. The pK_a of log k_{cat}/K_m profile with the mutant H346N is similar to that of the mutant H228 with the value of 8.0 ± 0.3. However, the mutant E384Q has a pK_a value of 6.0 ± 0.08, which is similar to the pK_a values obtained from the hydrolysis of Met-Pro.

Table 7. pK_a values of the log k_{cat} and log k_{cat}/K_m profiles for the hydrolysis of diethyl *p*-nitrophenyl phosphotriester.

Prolidase	pK_a	
	log k_{cat}/K_m	log k_{cat}
Wild-type	7.0 ± 0.06	7.1 ± 0.8
H228N	7.8 ± 0.08	7.7 ± 0.08
H346N	8.0 ± 0.3	N/A
E384Q	6.0 ± 0.08	N/A

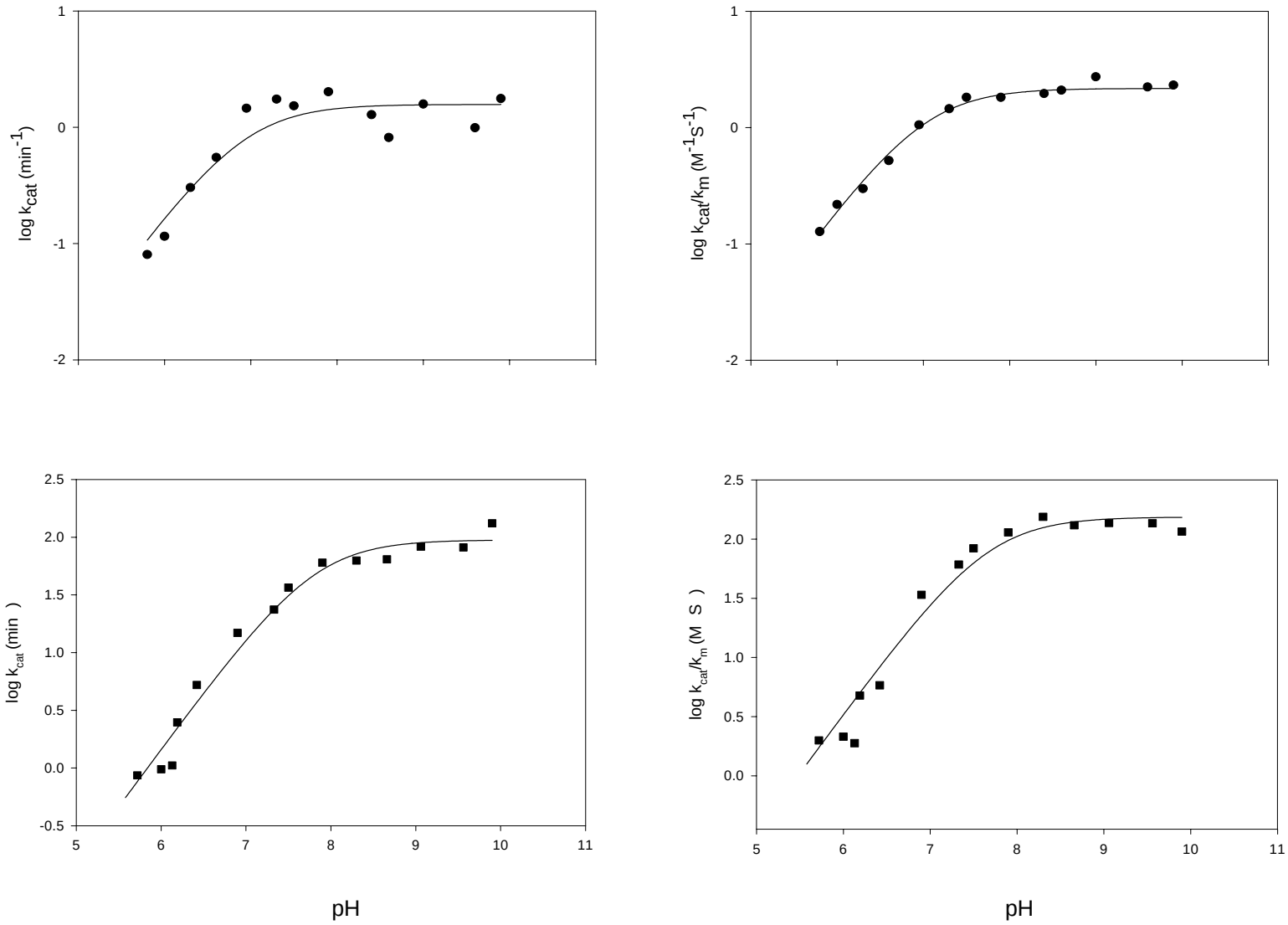

Figure 10: pH-rate profiles for the hydrolysis of diethyl *p*-nitrophenyl phosphotriester with wild-type (●) and H228N (■).

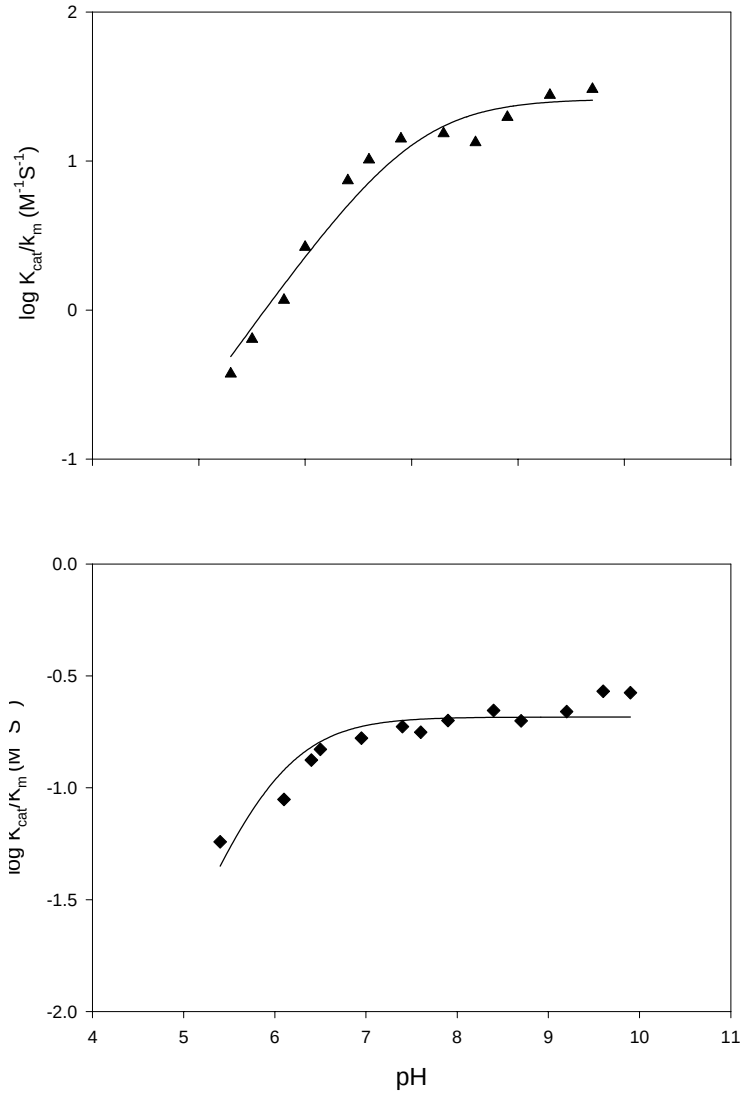

Figure 11: pH-rate profiles for the hydrolysis of diethyl *p*-nitrophenyl phosphotriester with H346N (▲) and E384Q (♦).

Discussion

Kinetic Parameters of the Wild-type and Mutants Prolidases for Dipeptide Substrates. The values of k_{cat}, K_m, and k_{cat}/K_m for the hydrolysis of Met-Pro by the mutants H228N and H346N are reduced. The result suggests that these histidines play an important role during the catalytic hydrolysis of peptides. However, the relative contributions of these histidines of MetAP and prolidase are different. The mutational analysis of His228, His346, and Glu384 of prolidase implies that these residues are not essential, but they facilitate catalysis. The more significant decrease of the catalytic activity of H346A compared to H346 suggests that the formation of a hydrogen bond to the substrate is an important factor for the enzyme-catalyzed reaction. The residual activity of mutants H178A (H346A in *E. coli* prolidase) and H79A (H228 in *E. coli* prolidase) of the MetAP from *E. coli* showed a 50-fold and 5 orders of magnitude reduction in activity in comparison to the wild-type enzyme [27]. The data demonstrated that the contribution of His178 is not critical for catalysis while His79 may help enzyme catalytic activity in a more productive manner. These results are different than observed effects upon mutation of His346 and His228 of the prolidase from *E. coli*. However, the contribution of the residues for hydrolysis may be different depending on the enzyme substrate even though the dinuclear metal clusters in the two enzymes are coordinated by identical sets of residues.

pH Dependence of Wild-type and Mutant Prolidase with Met-Pro Dipeptide. On the basis of the present results, it is concluded that the ionization states of specific amino acid residues are important. The enzyme requires three ionizations to catalyze proline

dipeptides. Two groups must be ionized at low pH, and one group at high pH with pK_a values of ~6 and ~9.5, respectively. The most logical candidate for the nucleophile that attacks the scissile bond of the proline dipeptides is the bridging water or hydroxide molecule between two metal ions. Therefore, an essential ionization with a pK_a value of ~6 within the active site of enzyme may be correlated to the deprotonation of the water molecule between two metal ions in the enzyme active site. The other candidate for ionization at low pH may be Glu384 with a similar pK_a value of the bridging water as shown in pH-rate profiles with mutant G384Q. Mutation of G384 resulted in ionization of one group at low pH in the enzyme-catalyzed reaction. The α-amino group within Xaa-Pro substrates appears to contribute to another ionization at high pH in the pH-rate profiles.

Mechanism of Prolidase for the Hydrolysis of Dipeptides. The X-ray crystal structures of the eMetAP- and *Pf*pro-inhibitor complexes provide some insight toward the role of the binuclear metal center for substrate hydrolysis and the binding of substrates within the enzyme active site. Combinations of the pH-rate profiles presented here, and the previous inhibitor-based studies suggest a potential mechanistic pathway. The mechanism in **Figure 12** is consistent with the pH-rate profiles for the *E. coli* prolidase and the structures of the eMetAP- and *Pf*pro-inhibitor complexes. However, for the active site structure of *Pf*pro in complex with the AHMH-Pro, caution should be applied in using this structure as a guide for how true substrates actually bind to the active site. There are two carbon atoms between the carbonyl oxygen from the proline moiety and the free amino group at the β-carbon, which make a longer distance than that

of Leu-Pro. Comparisons of the structures of eMetAP- and *Pf*pro-inhibitor complexes suggest that the carboxyl oxygen of the scissile bond may be between metal A and B, and His346 may have a hydrogen bond to the imide-nitrogen atom of the proline in the binding mode of Leu-Pro substrate in the active site of the prolidase from *E. coli*. The hydrogen bond may reasonably reduce the partial double-bond character and the activation barrier for the peptide bond as shown in investigations of MetAP and creatinase [30, 32]. The carboxyl oxygen of the scissile peptide bond interacts with metal A, and His228 has a hydrogen bond to the carboxyl oxygen. The N-terminus of the substrate coordinates to metal B as shown in the X-ray crystal structures of the eMetAP- and *Pf*pro-inhibitor complexes. However, the detail mechanism for how the usually positively charged N-terminus amino group coordinates to metal B should be investigated. Although there is no evidence for an obvious candidate to accept the proton from the N-terminus of Xaa-Pro substrates, a reaction mechanism suggested by G. Schürer et al [31] can be considered. The proton transfer to the bridging hydroxide between metal ions, the coordination of the N-terminus, and the coordination cleavage of the water molecule to metal B occur as a concerted process. Glu384 binds to the hydrogen from the bridging water to promote the attack of a nucleophile on the substrate.

The resulting tetrahedral intermediate is stabilized by chelation to metal A and by hydrogen bonds with His228 and His346. Proton transfer from the *gem*-diolate group to the nitrogen atom of the proline may facilitate releasing the proline- leaving group. When the binding product is released, a proton transfer from Glu384 to the N-terminus binding to metal B may enhance the releasing product bound to metal ions and regeneration of the substrate and hydroxide in the active site.

The possible mechanistic pathway can reasonably explain why the enzyme activity in pH-rate profiles at high pH is reduced. When the N-terminus of dipeptide is deprotonated at high pH, a lack of proton source may cause the drop of the enzyme activity because the N-terminus amino acid plays a role as a proton source to the releasing proline-leaving group. In addition, the positively charged N-terminus has a hydrogen bond to the hydroxide between metal ions. However, the detail mechanism of the regeneration step remains unclear. Enzyme kinetics and EPR spectroscopy studies with substrates and inhibitors is being sought to support this mechanism.

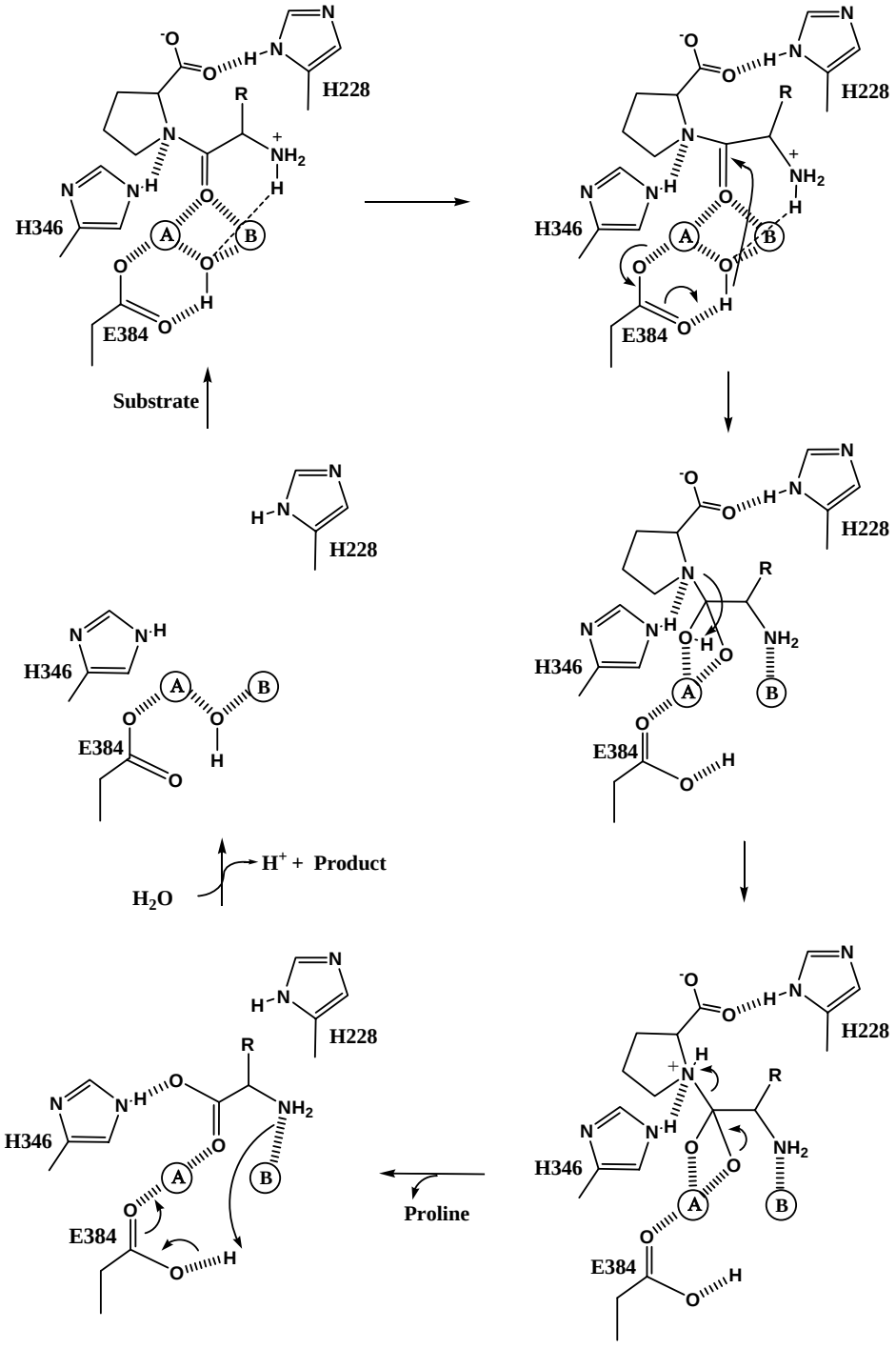

Figure 12: Proposed mechanism for *E. coli* prolidase catalysis. The R-group is a nonpolar side chain of proline dipeptide.

Kinetic Parameters and pH-rate Profiles of the Wild-type and Mutants Prolidases for Phosphotriester Substrates. The activity of the mutants H228N and H346N toward a phosphotriester substrate was increased. The results suggest that the H228 and H346 are not involved in the enzyme-catalyzed reaction. However, the reduction of the enzyme activity of the mutant G384Q suggests that G384 enhances the hydrolysis of phosphotriester substrates. The shapes of the pH-rate profiles for the hydrolysis of phosphotriester substrates, half-bell plots, are different to those of the pH-rate profiles for the hydrolysis of Met-Pro dipeptide. The most logical candidate that corresponds to an essential enzyme functionality with a pK_a value of ~6.5 in the pH-rate profiles is the bridging hydroxide between metal ions. However, the pK_a value measured from the plots are somewhat higher than those of the pH-rate profiles for hydrolysis of Met-Pro at the low pH. The measured pK_a value of the pH-rate profile for G384Q, matching the pK_a values for the hydrolysis of Met-Pro at the low pH, implies that G384 is involved in ionization of the water molecule bound to metal ions.

Mechanism of Prolidase for the Hydrolysis of Phosphotriesters. Although the kinetics of phosphotriester hydrolysis show different pH-rate profiles than observed for the Xaa-Pro substrate, an assumption concerning a general base mechanism that proceeds via an attack of a nucleophile to the phosphorus center of the phosphotriester substrate can be considered. A possible mechanism is proposed in **Figure 13**. The suggested mechanism is similar to that of the Xaa-Pro dipeptide hydrolysis. The phosphoryl oxygen of the phosphotriester substrate is bound and polarized by the metal ions, and the metal-bound hydroxide attacks the phosphorus atom. However, since the *p*-

nitrophenyl group (pK_a is ~10 in water) is a good leaving group, the proton transfer from any proton source may be not necessary. It might be related to no activity reduction at high pH in the pH-rate profiles for phosphotriester hydrolysis. However, a proton acceptor from G384 in the regeneration step remains unclear.

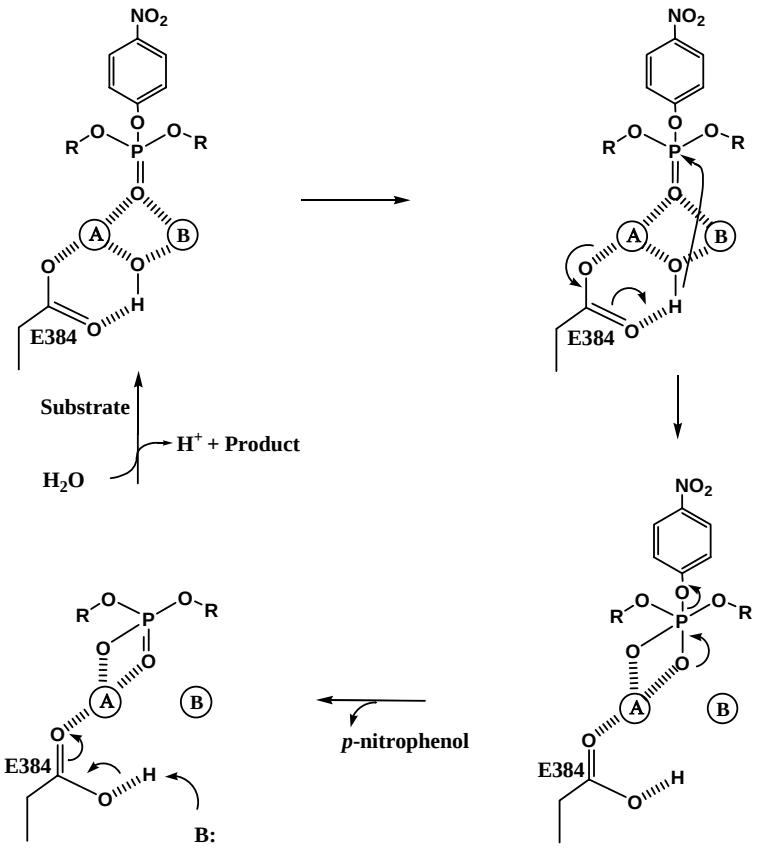

Figure 13. Proposed mechanism for phosphotriester hydrolysis catalyzed by the prolidase.

CHAPTER IV

CONCLUSIONS

The PepQ prolidase from *Escherichia coli* catalyzes the hydrolysis of dipeptides substrates with proline residues at the C-terminus. Significant catalytic activity occurred with dipeptides containing nonpolar amino acids at the N-terminal position. The enzyme also catalyzes the stereoselective hydrolysis of phosphate and phosphonate esters but the turnover numbers for the dipeptides are significantly greater than for the phosphorus containing esters. In addition, the PepQ prolidase can be utilized for the kinetic resolution of racemic phosphate esters.

The activity of the mutants H228N, H346N, and E384Q toward Met-Pro was somewhat reduced. The mutational analysis of His228, His346, and Glu384 of prolidase implies that these residues are not essential, but they facilitate catalysis. Prolidase requires three ionizations to catalyze proline dipeptides. Two groups must be ionized at the low pH, and one group at the high pH with pK_a values of ~6 and ~9.5, respectively. The comparison of the enzyme activity with 1-(1-oxopropyl)-L-proline and Ala-Pro suggests that the α-amino group of Xaa-Pro dipeptides plays an important role for the enzyme-catalyzed reaction. Combinations of the present pH-rate profile results and the previous inhibitor-based studies suggest a potential mechanistic pathway. However, the detail mechanism of the regeneration step remains unclear. The activity of the mutants H228N and H346N toward a phosphotriester substrate was increased. The results suggest that the H228 and H346 are not involved in the enzyme-catalyzed reaction.

However, the reduction of the enzyme activity of the mutant G384Q suggests that G384 enhances the hydrolysis of phosphotriester substrates. A possible mechanism is proposed and the mechanism is similar to that of the Xaa-Pro dipeptide hydrolysis. However, a proton acceptor from G384 in the regeneration step remains unclear.

REFERENCES

[1] Schrag, J.D., Li, Y., Wu, S., and Cygler, M. (1991). *Nature*. *351*, 761-764.

[2] Kabashima, T. Fujii., Hamasaki, M., Ito, Y., and T. Yoshimoto, K. (1999). *Biochimica et Biophysica Acta*. *1429*, 516-520.

[3] Bazan, J.F., Weaver, L.H., Roderick, S.L., and Matthews, B.W. (1994). *Proc. Natl. Acad. Sci. USA*. 91, 2473-2477.

[4] Lowther, W. T., and Matthews, B.W. (2000). *Biochimica et Biophyscia Acta*. *1477*, 157-167.

[5] Jackson, S., Dennis, A., and Greenberg, M. (1975). *Can. Med. Assoc*. J. *113*, 759-763.

[6] Booth, M., Jennings, V., Fhaolain, N.I., and O'Cuinn, G. (1990). *J. Dairy Res. 57*, 245-254.

[7] Cheng, T.-C., Harvey, S.P., and Chen, G.L. (1996). *Appl. Envrion. Microbiol*. *62*, 1636-1641.

[8] Ghosh, M., Grunden, A.M., Dunn, D.M., Weiss, R., and Adams, M.W.W. (1998). *J. Bacteriol. 180*, 4781-4789.

[9] Maher, M.J., Ghosh, M., Grunden, A.M., Menon, A.L., Adams, M.W., Freeman, H.C., and Guss, J.M. (2004). *Biochemistry. 43*, 2771-2783.

[10] Mittal, S., Song, X., Vig, B.S., Landowski, C.P., Kim, I., Hilfinger, J.M., and Amidon, G.L. (2005). *Molecular Pharmaceutics*. *2*, 37-46.

[11] Park, M.S., Hill, C.H., Li, Y., Hardy, R.K., Khanna, H., Khang, Y.H., and Raushel, F.M. (2004). *Achiv. Biochem. Biophys. 429*, 224-230.

[12] Ecobichon, D.J. (1995) in *Casarett and Doull's Toxicology*: The Basic Science of Posions (Klaassen, C.D, Ed.), pp. 655-666, McGraw Hill, New York, NY.

[13] Mazur, A. (1946). *J. Biol. Chem*. *164*, 271-289.

[14] DeFrank, J.J., Beaudry, W.T., Chang, T.-C., Harvey, S.P., Stroup, A.N., and Szafraniec, L.L. (1993). *Chem. Biol. Interact. 87*, 141-148.

[15] Landis, W.G., and DeFrank, J.J. (1990). *Adv. Appl. Biotechnol. 4*, 183-201.

[16] Cheng, T.-C., Liu, L., Wang, J., Wu, J., DeFrank, J.J., Anderson, D.M., Rastogi, V.K., and Hamilton, A.B. (1997). *J. Ind. Microbiol. 18*, 49-55.

[17] Hill, C.M., Wu, F., Cheng, T.-C., DeFrank, J.J., and Raushel, F.M. (2000). *Biochem. Med. Chem. Latter. 10*, 1285-1288.

[18] Hill, C.M., Li, W.-S., Cheng, T.-C., DeFrank, J.J., and Raushel, F.M. (2001). *Bioorg. Chem*, *29*, 27-35.

[19] Hong, S.B, and Raushel, F.M. (1999). *Biochemistry*. *38*, 1159-1165.

[20] Koizumi, T., Kobayashi, Y., Amitani, H., and Yoshii, E. (1977). *J. Org. Chem*. *42*, 3459-3460.

[21] Donarski, W.J., Dumas, D.P., Heitmeyer, D.P., Lewis, V.E., and Raushel, F.M. (1989). *Biochemistry*. *28*, 4650-4655.

[22] Wu, F., Li, W.-S., Chen-Goodspeed, M., Sogorb, M. A., and Raushel, F.M. (2000). *J. Am. Chem. Soc. 122*, 10206-10207.

[23] Yoshimoto, T., Orawski, A.T., and Simmons, W.H. (1994). *Achiv. Biochem. Biophys. 1*, 28-34.

[24] Dumas, D.P., Durst, H.D., Landis, W.G., Raushel, F.M., and Wild, J.R. (1989). *Arch. Biochem. Biophys. 164*, 1137.

[25] Li, W.S., Lum, K.T., Chen-Goodspeed, M., Sogorb, M. A., and Raushel, F.M. (2001). *Bioorg. Med. Chem. 9*, 2083-2091.

[26] Roderick, S.L., and Matthews, B.W. (1993). *Biochemistry*, *32*, 3907-3912.

[27] Lowther, W.T., Orville, A.M., Madden, D.T., Lim, S., Rich, D.H., and Matthews, B.W. (1999) *Biochemistry. 38*, 7678-7688.

[28] Cottrell, G.S., Hyde, R.J., Lim, J., Parsons, M.R., Hooper, N.M., and Turner, A.J. (2000) *Biochemistry. 39*, 15129.

[29] Lowther, W.T., Zhang, Y., Sampson, P.B., Honek, J.F., and Matthews, B.W. (1999). *Biochemistry*. *38*, 14810-14819.

[30] Ghosh, M., Grunden, A.M., Dunn, D.M., Weiss, R., and Adams, M.W.W. (1998). *J. Bacteriol. 180*, 4781-4789.

[31] Schürer, G., Lanig, H., and Clark, T. (2004). *Biochemistry*. *43*, 5414-5427.

[32] Coll, M., Knof, S.H., Ohga, Y., Messerschmidt, A., Huber, R., Moellering, H., Russmann, L., and Schumacher, G. (1990) *J. Mol. Biol*. *214*, 597-610.

VITA

Min Sun Park was born on June 7, 1971 in Seoul, capital of South Korea. He earned his degree of Bachelor of Science in January 1999 from Sogang University. He was a research associate in Sogang University and Korea Institute of Science and Technology during 1999 to May 2001. He earned his Master of Science specializing in chemistry in August 2005, from Texas A&M University.

Permanent mailing address: 102-2501 Samik Apartment, Myunmock Jungrang
Seoul, Korea 131-200